Commensurability-Dependent Transport of a Wigner Crystal in a Nanoconstriction

D. G. Rees,[1,*] H. Totsuji,[1,2] and K. Kono[1]

[1]Low Temperature Physics Laboratory, RIKEN, Wako 351-0198, Japan

[2]Graduate School of Natural Science and Technology, Okayama University, Tsushimanaka 3-1-1, Okayama 700, Japan

(Received 29 November 2011; published 25 April 2012)

We present the first transport measurements of a classical Wigner crystal through a constriction formed by a split-gate electrode. The Wigner crystal is formed on the surface of superfluid helium confined in a microchannel. At low temperatures, the current is periodically suppressed with increasing split-gate voltage, resulting in peaklike transport features. We also present the results of molecular dynamics simulations that reproduce this phenomenon. We demonstrate that, at the split-gate voltages for which the current is suppressed, the electron lattice is arranged such that the stability of particle positions against thermal fluctuations is enhanced. In these configurations, the suppression of transport due to interelectron Coulomb forces becomes important.

DOI: 10.1103/PhysRevLett.108.176801 PACS numbers: 73.20.Qt, 45.50.Jf, 73.23.−b, 85.30.Hi

The transport of particles through constrictions is of fundamental importance in many physical systems. For noninteracting Fermi gases in quantum point-contacts, electron conductance is quantized in units of $G_0 = 2e^2/h$ [1]. For systems in which interactions between particles are significant, a rich variety of dynamical phenomena such as jamming and pinning may be observed at bottlenecks. Such processes are important at the microscopic scale, in systems such as vortex matter in superconducting films [2] and colloids in microchannels [3], as well as in macroscopic systems such as granular hoppers [4] and pedestrians negotiating doorways [5]. However, despite occurring commonly in nature, the transport of interacting particles through constrictions remains poorly understood. Here we report novel transport dynamics observed in a strongly correlated electron system, formed on the ultraclean surface of liquid helium, passing through a constriction. With the aid of numerical simulations, we demonstrate that the electron transport depends on the geometrical arrangement of particles close to the constriction. Remarkably, under certain circumstances, this behavior leads to a reduction of current with increasing constriction width. Although we are aware of no previous demonstration of this effect, similar behavior should be observable in many other strongly correlated classical systems and may also be important in quantum wires when the effects of Coulomb interaction are significant [6]. As electrons on helium have been proposed as quantum bits with long coherence times, the manipulation of electron lattices may also be important for quantum information processing [7–9].

Surface-state electrons (SSEs) on the surface of helium form a unique example of a classical, rather than quantum, two-dimensional electron system [10]. Below 2 K, electrons occupy the ground state of motion perpendicular to the surface, ''floating'' 11 nm above the liquid, but are free to move in the parallel plane with a mobility of $\mu \sim 10^6$ cm^2/V s at 1 K [11]. For typical electron densities ($n \approx 10^6$–10^9 cm^{-2}), the system is nondegenerate and, as the relative permittivity of the liquid helium is close to unity ($\varepsilon = 1.054$), the Coulomb interaction between electrons is essentially unscreened. The system undergoes a transition from a liquidlike state to a triangular lattice, the Wigner crystal (WC), for $\Gamma \gtrsim 130$, where $\Gamma = e^2\sqrt{\pi n}/4\pi\varepsilon\varepsilon_0 k_B T$ is the ratio of the Coulomb energy per electron to the average kinetic energy [12]. Here, e is the elementary charge, ε_0 the vacuum permittivity, T the temperature, and k_B the Boltzmann constant. This expression gives the melting temperature $T_m \simeq 1$ K for $n = 2 \times 10^9$ cm^{-2}.

We have previously studied the transport of SSEs in a split-gate device in the electron liquid regime [13]. As the constriction was opened, the conductance increased in a stepwise manner. Each conductance step was attributed to an increase in the number of electrons able to pass side-by-side through the constriction, as confirmed by recent numerical investigations [14]. Here, we investigate electron transport in a similar device at lower temperatures, at which the electrons form a WC.

The sample used in this experiment, shown in Fig. 1(a), was similar to those used in previous experiments [13], which were fabricated on a silicon wafer by optical lithography. Two gold layers of 100 nm thickness are separated by a 1.7-μm-thick insulating layer made of hard-baked photoresist. The lower metal layer forms the *split-gate* electrode of 2.6 μm separation and the left and right *reservoir* electrodes. The upper metal layer forms a *guard* electrode shaped so as to define two arrays of microchannels, which serve as electron reservoirs, separated by a short channel of 10 μm width, at the center of which is the split-gate electrode. The microchannel reservoirs, which are not shown in Fig. 1(a), are geometrically identical to those used previously [13]. The microchannels are filled by the capillary action of superfluid ^{4}He. The dc potentials V_r, V_{gt}, and V_{gu} are applied to the reservoir, split-gate and

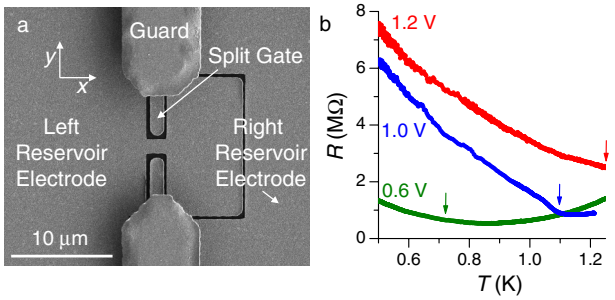

FIG. 1 (color online). (a) Scanning electron micrograph image of the constriction between the two SSE reservoirs. (b) Resistance of the electron system (R) against T for $V_r = V_{gt} = 1.2$, 1.0 and 0.6 V. Arrows indicate the melting temperature of the Wigner solid calculated assuming a saturated electron density, taking into account the experimentally observed offset in V_{gu}.

guard electrodes, respectively. SSE are generated by a tungsten filament above the sample. A small ac voltage V_{in} with the frequency $f_{in} = 200$ kHz is superimposed on the right reservoir electrode to drive electrons between the two reservoirs through the constriction. The peak ac current I and the electron system resistance R are determined by the phase-sensitive measurement of the ac voltage induced on the left reservoir electrode according to a lumped-RC circuit model [15].

For $V_r = 0$ V, it is found that the surface of the helium can only be charged when $V_{gu} < -0.3$ V. In our previous devices, a similar effect was attributed to an offset in the guard electrode potential that may have been due to surface charging effects or contact, or patch, potential differences. We therefore write the effective value of the guard electrode potential as $V^{\star}_{gu} = V_{gu} + V^{0}_{gu}$, where $V^{0}_{gu} = 0.3$ V. The maximum (saturated) electron density in the reservoirs (n_s) is then given by $n_s = \varepsilon\varepsilon_0(V_r - V^{\star}_{gu})/ed$. For all the following results, $V_{gu} = 0$ V and $V^{\star}_{gu} = 0.3$ V.

The electron density may also be estimated by measuring the temperature dependence of R. For the electron liquid, resistivity decreases with decreasing T, while in the WC regime the formation of a depression of the helium surface beneath each localized electron leads to an increase in resistivity with decreasing T [16]. In Fig. 1(b), we show R against T for three V_r values. In each case, $V_r = V_{gt}$. Under this condition, the dependence of I on V_{gt} is negligible, indicating that the widely open constriction has a small resistance, and R is determined mainly by the resistance of the electron system in the reservoirs. For $V_r = 1.2$ V, for which we expect $n_s = 3.1 \times 10^9$ cm^{-2} and $T_m = 1.25$ K, R increases as T decreases, indicating that the electron system is already in the WC regime at $T = 1.25$ K. For $V_r = 1.0(0.6)$ V, we obtain $n_s = 2.4(1.0) \times 10^9$ cm^{-2} and $T_m = 1.10(0.72)$ K. These values for T_m lie close to the minima in R associated with the formation of the WC. These measurements confirm that the electron system crystallizes at low temperatures and that our estimate of the electron density in the reservoir microchannels is close to the true value.

The results of sweeping V_{gt} for $V_r = 1.2$ V at different temperatures are shown in Fig. 2(a). Here, we show the normalized current I/I_{max} for V_{gt} values between -0.5 and -2.0 V, where I_{max} is the current measured for $V_{gt} = -0.5$ V. We note that I_{max} decreases with decreasing temperature; for $T = 1.2(0.7)$ K, $I_{max} = 318(175)$ pA. This trend is in agreement with the increasing resistance shown in Fig. 1(b) for $V_r = 1.2$ V. For $T = 1.2$ K, above the split-gate voltage threshold of current flow (V^{th}_{gt}), the current initially increases in a series of steps, as reported previously [13]. The first two steps are clear, while the third is only weakly visible. With decreasing T, the steps unexpectedly develop into an oscillatory structure, which results in peaklike features, the first two of which are clearly visible. The maximum temperature at which the first peak can be resolved is 0.95 K. Assuming a saturated electron density, this corresponds to $\Gamma = 164$.

The separation between the current steps (or peaks at low T) is $\Delta V_{gt} \approx 200$ mV. Following our previous analytical approach [13], the electrostatic potential on the helium surface at the center of the constriction (V_b) is related to V_{gt} by a constant β. The change in V_b between the steps is therefore $\Delta V_b = \beta \Delta V_{gt}$. β may be estimated by assuming that, for a saturated density, the current threshold is reached when $V_b = V^{\star}_{gu}$. By also assuming the effect of V_{gu} on V_b to be negligible, we can write $\beta(V_r - V^{th}_{gt}) = V_r - V^{\star}_{gu}$. As $V_r - V^{th}_{gt} = 2.65$ V, $\beta = 0.34$, and $\Delta V_b = 68$ mV.

In Fig. 2(b), we compare I/I_{max} for $T = 1.2$ and 0.7 K. Over the course of the measurement, which takes several hours, the current threshold is typically observed to drift by a small amount. This drift does not depend on temperature and is most probably due to the loss (gain) of a small

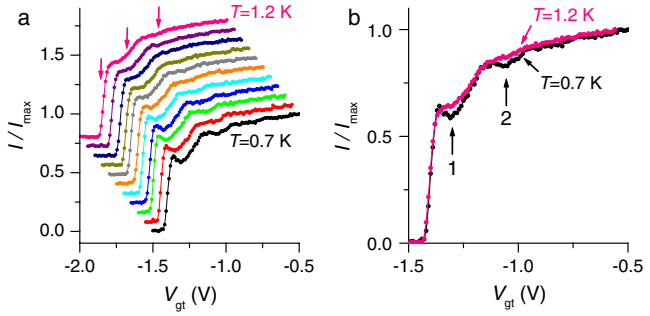

FIG. 2 (color online). (a) I/I_{max} against V_{gt} for temperatures between 0.7 and 1.2 K in 50 mK steps. Here $V_r = 1.2$ V and $V_{in} = 2$ mV$_{pp}$. With increasing T, each data set is shifted -50 mV horizontally and 0.08 vertically for clarity. Arrows mark the steplike increases in current at 1.2 K. (b) Data for $T = 1.2$ and 0.7 K with no vertical shift. The 1.2 K data are shifted by -60 mV horizontally. The numbered arrows indicate points at which the current is suppressed.

number of electrons to (from) the thin helium film covering the surface of the guard electrode [13]. Therefore, the data obtained at 1.2 K is shifted by $V_{\rm cor} = -60$ mV horizontally to aid comparison. This change in $V_{\rm gt}^{\rm th}$ relative to V_r is $|V_{\rm cor}|/(V_r - V_{\rm gt}^{\rm th}) \sim 2\%$. Because the corresponding change in V_b, and thus n, is of the same magnitude, this shift represents negligibly small changes in n and Γ. The plot reveals that the peaks appear to be formed by the suppression of current at low temperatures at points between the stepwise increases in current. In numerical simulations of our devices, Araki and Hayakawa have confirmed that each current step corresponds to the addition of an electron "row" across the constriction, and that each step is smoothed due to temporal fluctuations in the number of rows [14]. This number was most stable at the center of each step plateau. In Fig. 2(b), this occurs at the points labeled 1 and 2. We therefore conclude that the current is suppressed when the number of electrons across the constriction is close to 1 or 2.

In Fig. 3(a), we show the results of sweeping $V_{\rm gt}$ between 0.5 and -1.5 V for decreasing V_r at $T = 0.7$ K. Here, $I_{\rm max}$ is the current measured for $V_{\rm gt} = 0.5$ V. $V_{\rm gt}^{\rm th}$ increases in equal steps with each decrease in V_r, indicating that for each $V_{\rm gt}$ sweep, the helium surface is saturated [13]. $I_{\rm max}$ increases with each decrease in V_r, as expected when the decreasing density of the WC leads to a decrease in resistivity. For $V_r = 1.15(0.75)$ V, $I_{\rm max} = 224(575)$ pA. The lowest value of V_r at which the first current peak is visible is $V_r = 1.05$ V, for which $n_s = 2.6 \times 10^9$ cm^{-2} and $\Gamma = 204$. The reason for the discrepancy between the Γ values at which the peak is first observed is not clear, although inaccuracy in the estimated value of n_s may cause such a disagreement. We also note that n_s is the electron density in the reservoirs, rather than at the constriction which is more difficult to quantify. The additional structures at higher $V_{\rm gt}$ in Fig. 3(a) are not understood but could be related to the sudden increase in the effective width of the constriction when electrons begin to flow above the split gates.

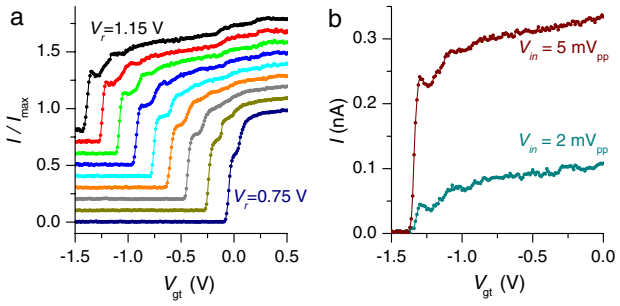

FIG. 3 (color online). (a) $I/I_{\rm max}$ against $V_{\rm gt}$ for V_r values between 1.15 and 0.75 V, $T = 0.7$ K and $V_{\rm in} = 2$ mV$_{\rm pp}$. With increasing V_r, each data set is shifted 0.1 vertically. No horizontal shift is added to the data. (b) I against $V_{\rm gt}$ for $V_{\rm in} = 2$ mV$_{\rm pp}$ and 5 mV$_{\rm pp}$, $T = 0.5$ K and $V_r = 1.2$ V.

In Fig. 3(b), we show I against $V_{\rm gt}$ for two $V_{\rm in}$ values at $T = 0.5$ K and $V_r = 1.2$ K. The oscillatory structure remains for $V_{\rm in} = 5$ mV$_{\rm pp}$, for which the current at $V_{\rm gt} = 0$ V is similar to $I_{\rm max}$ for $T = 1.2$ K in Fig. 2(a). This indicates that the appearance of the oscillations does not depend intrinsically on the magnitude of I. However, we note that the smoothing of these features is observed for $V_{\rm in} \gtrsim 10$ mV$_{\rm pp}$, which is comparable to ΔV_b. We attribute this effect to the strong modulation of the electrostatic potential energy of the electron system, and thus the electron density at the constriction, over each ac cycle.

We have also performed molecular dynamics simulations of electrons at a constriction. The system of 192 electrons of charge $-e$, free electron mass m_e and position $\mathbf{R} = (x, y)$ is confined to a channel-like domain with a constriction at the center. The Hamiltonian is

$$\sum_i \frac{m_e}{2}\left(\frac{d\mathbf{R}_i}{dt}\right)^2 + \sum_{i>j} \frac{e^2/4\pi\varepsilon_0}{|\mathbf{R}_i - \mathbf{R}_j|} - \sum_i eV_{\rm ext}(\mathbf{R}_i), \qquad (1)$$

$$V_{\rm ext}(\mathbf{R}) = V_{\rm gu}^s \tanh\left(\frac{y^2}{(\eta l_0)^2}\right) + V_{\rm gt}^s \frac{1}{1 + (x/\xi l_0)^2}, \qquad (2)$$

where $V_{\rm ext}$ is the confining potential. The shape of the channel is determined by $V_{\rm gu}^s = -325$ mV, the constants $\xi = 1$ and $\eta = 1.6$ and the length scale $l_0 = 0.665$ μm. The constriction profile is controlled by $V_{\rm gt}^s$. The fundamental cell is $|x| \le 5l_0$ and $|y| \le l_0$ with a periodic boundary condition in x. Electrons are distributed approximately in $|y| \le 0.7l_0$ giving $n \sim 3.1 \times 10^9$ cm^{-2}.

A small dc bias of $V_s = 0.217$ mV is applied to drive the charges in the positive x direction. The effect of elastic scattering by helium atoms and ripplons is simulated by multiplying the factor $\exp(-\Delta t/\tau)$ to the x component of the average velocity after each step of integration Δt, keeping the velocity relative to the average velocity unchanged. The mean free time $\tau = 9$ ps ($\mu = 1.5 \times 10^4$ cm^2/V s) is chosen to obtain the open current $I_{\rm max}^s = 230$ pA which is of the same order of magnitude as that obtained in the experiment. Since our system is a straight channel when the constriction is removed, μ much smaller than 10^6 cm^2/V s gives $I_{\rm max}$ comparable to the experiment. The temperature is controlled by scaling the kinetic energy relative to the average velocity. The system conductance is calculated as $G_s = I_s/V_s$ at different temperatures and $V_{\rm gt}^s$ values. Further details will be presented elsewhere [17].

In Fig. 4(a), we show G_s as a function of $V_{\rm gt}^s$ for different Γ values. In all three cases, the conductance becomes zero below $V_{\rm gt}^s \approx -120$ mV. Above this threshold, oscillations in G_s are visible for $\Gamma = 98$ and are more pronounced for $\Gamma = 131$. The oscillation period is $\Delta V_{\rm gt}^s \approx 20$ mV, which is similar in magnitude to the experimental value of ΔV_b. In Fig. 4(b), we show superposed images of particles for

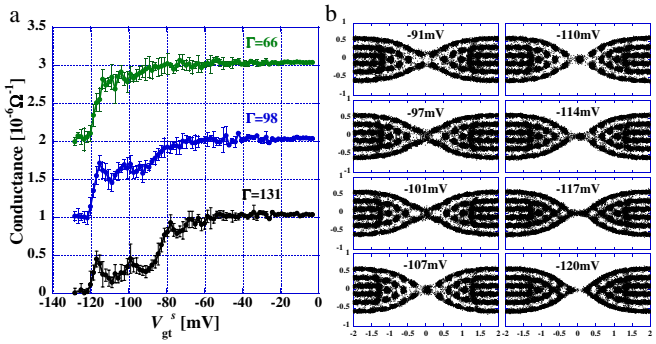

FIG. 4 (color online). Results of molecular dynamics simulations. (a) Conductance G_s against $V_{\rm gt}^s$ for different Γ values. Data for $\Gamma = 98$ and 66 are shifted by 1 and $2 \times (\mathrm{M}\Omega)^{-1}$, respectively. (b) Superposed images for $\Gamma = 131$ and different $V_{\rm gt}^s$ values. $V_{\rm gt}^s$ values are shown on each plot. The unit of length is l_0.

$\Gamma = 131$ and several different $V_{\rm gt}^s$ values obtained at a fixed time interval over the same duration.

At $V_{\rm gt}^s = -107$ mV, where we observe a strong suppression of conductance, images of electrons around the constriction form a symmetric latticelike configuration with one electron at the center, surrounded by four electrons. When $V_{\rm gt}^s$ approaches -117 mV, the images become more blurred and, in particular, the fluctuation in the position of the central electron increases in x. Around $V_{\rm gt}^s = -117$ mV, the central electron's fluctuation reaches a maximum corresponding to the peak in G_s. At $V_{\rm gt}^s = -120$ mV, this electron begins to be localized to the left of the constriction and we observe almost no passage of electrons through the constriction. Similarly, the peak in G_s around $V_{\rm gt}^s = -97$ mV coincides with an increase in particle motion and the suppression around $V_{\rm gt}^s = -91$ mV corresponds to localized and distinct particle positions. In this case, two electron rows are almost fully formed at the constriction without the central electron.

For $V_s = 0$, we obtain images (not shown) qualitatively similar to those for $V_s = 0.217$ mV in Fig. 4(b). Since the energy associated with the latter is still of the same order of magnitude as the thermal energy $k_B T \sim 0.08$ meV, we find it reasonable that the thermal fluctuations in particle positions are closely related to the conductance of the system, in accordance with the fluctuation-dissipation theorem for linear response [18].

The simulations have revealed that, when the geometry determined by $V_{\rm gt}^s$ allows a commensurate, highly ordered and symmetric configuration, the positions of electrons around the constriction become stable against thermal fluctuations and the conductance is suppressed. This increased stability may be regarded as an effective increase in Γ for the particles close to the constriction. A similar modulation of Γ as a function of confinement width has been observed in numerical simulations of classical charges in a straight quasi-one-dimensional potential [19]. Related studies have shown that at low temperatures (large Γ) the WC should become pinned in saddle-point potentials similar to ours [20]. We therefore interpret the current suppression as signifying the onset of pinning at the constriction when the lattice configuration promotes the stability of the WC.

We note that the Γ values at which the oscillations appear in the experiment and simulation are different. Because Γ is defined for the bulk electron system away from the constriction, this discrepancy is most likely due to differences in the constriction geometry in the two systems, which influences the interelectron separation and so interaction strength. However, the observation of current oscillations in both the experiment and the simulation indicates that they are a fundamental phenomenon and so should be observable in other systems of strongly correlated particles passing through bottlenecks.

In conclusion, we have performed the first investigation of the transport of a classical Wigner crystal on liquid helium through a constriction. Comparison with numerical simulations reveals that an oscillation of the electron current, which appears as the constriction is opened, occurs due to changes in the arrangement of the electron lattice within the confining potential. As electrons on helium are a model many-body system, our results are applicable to the transport of many other strongly correlated systems in confined geometries.

We thank H. Ikegami, P. Leiderer, M. Araki, H. Hayakawa, and F. Nori for useful discussions. This work was partially supported by KAKENHI. The RIKEN Integrated Cluster of Clusters (RICC) facility was used to perform the simulation. D. G. R. was supported by the RIKEN FPR Program.

*drees@riken.jp

[1] B. J. vanWees, H. van Houten, C. W. J. Beenakker, J. G. Williamson, L. P. Kouwenhoven, D. van der Marel, and C. T. Foxon, Phys. Rev. Lett. **60**, 848 (1988).
[2] K. Yu, M. B. S. Hesselberth, P. H. Kes, and B. L. T. Plourde, Phys. Rev. B **81**, 184503 (2010).
[3] D. Genovese and J. Sprakel, Soft Matter **7**, 3889 (2011).
[4] K. To, P.-Y. Lai, and H. K. Pak, Phys. Rev. Lett. **86**, 71 (2001).
[5] D. Helbing, I. Farkas, and T. Vicsek, Nature (London) **407**, 487 (2000).
[6] W. K. Hew, K. J. Thomas, M. Pepper, I. Farrer, D. Anderson, G. A. C. Jones, and D. A. Ritchie, Phys. Rev. Lett. **102**, 056804 (2009).
[7] P. M. Platzman and M. I. Dykman, Science **284**, 1967 (1999).
[8] S. A. Lyon, Phys. Rev. A **74**, 052338 (2006).
[9] D. I. Schuster, A. Fragner, M. I. Dykman, S. A. Lyon, and R. J. Schoelkopf, Phys. Rev. Lett. **105**, 040503 (2010).

[10] *Two-dimensional Electron Systems on Helium and Other Cryogenic Substrates*, edited by E. Andrei (Kluwer Academic, Dordrecht, 1997).
[11] C. C. Grimes and T. R. Brown, Phys. Rev. Lett. **32**, 280 (1974).
[12] C. C. Grimes and G. Adams, Phys. Rev. Lett. **42**, 795 (1979).
[13] D. G. Rees, I. Kuroda, C. A. Marrache-Kikuchi, M. Höfer, P. Leiderer, and K. Kono, Phys. Rev. Lett. **106**, 026803 (2011).
[14] M. Araki and H. Hayakawa, (arXiv:1104.4854).
[15] Y. Iye, J. Low Temp. Phys. **40**, 441 (1980).
[16] Yu. P. Monarkha and V. B. Shikin, Zh. Eksp. Teor. Fiz. **68**, 1423 (1975); Sov. Phys. JETP **41**, 710 (1975).
[17] H. Totsuji (to be published).
[18] R. Kubo, Rep. Prog. Phys. **29**, 255 (1966).
[19] G. Piacente, I. V. Schweigert, J. J. Betouras, and F. M. Peeters, Phys. Rev. B **69**, 045324 (2004).
[20] G. Piacente and F. M. Peeters, Phys. Rev. B **72**, 205208 (2005).